Groundwater geochemistry of a nitrate contaminated agricultural site

Hiroki Amano・Kei Nakagawa・Ronny Berndtsson

H. Amano ・K. Nakagawa (✉)*

Graduate School of Fisheries and Environmental Sciences, Nagasaki University, 1-14 Bunkyo-machi, Nagasaki 852-8521, Japan

e-mail: kei-naka@nagasaki-u.ac.jp

Tel.: +81 95 819 2763; fax: +81 95 819 2763

R. Berndtsson

Division of Water Resources Engineering & Center for Middle Eastern Studies, Lund University, Box 118 SE-221 00 Lund, Sweden

*Corresponding author

Abstract

Groundwater samples were collected from several depths down to 50 m below soil surface to investigate vertical profiles of NO_3^- and hydrogeochemical characteristics of the experimental site. The experimental site is located in the Shimabara City, Nagasaki, Japan, where nitrate contamination in groundwater has occurred due to intensive

agricultural activities. The transition zone between dissolved ions was found between specific depths caused by differences in the permeability of soil layers. Though NO_3^- concentration decreased significantly in the transition zone, the entire soil depth exceeded permissible level (50 mg L^{-1}) for drinking purposes. Comparing the temporal NO_3^- fluctuation above the transition zone with that of the below, distinct fluctuations were observed depending on sampling campaign. High rainfall amounts typically lead to initial decrease in NO_3^- concentration for the shallow groundwater. After some time, however, increase in NO_3^- concentration occurred due to leaching of accumulated NO_3^- in the soil matrix. This indicated that temporal NO_3^- fluctuation is mainly controlled by natural impact and occurring crop system. Results of principal component analysis suggested that application of chemical fertilizers ($(NH_4)_2SO_4$, NH_4NO_3, and KCl), dissolution of minerals (feldspar, calcite and dolomite), and ion exchange are the predominant factors resulting in the observed vertical groundwater chemistry. The relative magnitude between these three principal component scores changed across the transition zone. Below the transition zone, groundwater geochemistry reflected application of NH_4NO_3 and KCl fertilizer and dissolution of albite and orthoclase.

Keywords

Groundwater, Nitrate contamination, Vertical profile, Nitrate fluctuation, Principal component analysis

Introduction

Nitrate contamination in groundwater is often caused by non-point sources originating from intensive agricultural activities. The high solubility with nitrate fertilizers and low retention capacity of soils increase the

problem. In line with this, spatial investigations have been carried out over large areas to map pollution extent and excessive NO_3^- concentrations exceeding the permissible 50 mg L^{-1} for drinking water recommended by the World Health Organization (WHO 2011; Jalali 2011; Nemčić-Jurec et al. 2013; Ağca et al. 2014; Esmaeili et al. 2014). Investigations have also revealed the vertical distribution of NO_3^- concentration (Liu et al. 2005; Ju et al. 2006; Chandna et al. 2011; Esmaeili et al. 2014). The predominant feature of these investigations was that NO_3^- concentration decreased with increasing groundwater depth (e.g, Kundu et al. 2009). The results suggest that groundwater for drinking purposes should be collected at large depths in order to avoid nitrate contamination (Chandna et al. 2011). NO_3^- concentration varies in wide range at shallow groundwater depth because it may be influenced by many processes such as pumping or infiltration of water through the crop root zone. Deeper groundwater levels are, however, affected by fewer processes and pure diffusion of free NO_3^- (Liu et al. 2005). However, NO_3^- concentration usually changes drastically at a specific soil depths due to occurrence of impermeable geologic layers (Choi et al. 2010). Local factors determine the exact occurrence of these factors.

Temporal NO_3^- fluctuations are significantly related application rates of N-fertilizer (Derby et al. 2009), rainfall events (Sorensen et al. 2015), and mixing of shallow groundwater due to pumping (Ki et al. 2015). Moreover, the time lag between nitrate application and NO_3^- reaching the groundwater is determined soil type, hydrogeological, and climatic properties (Fenton et al. 2011). Therefore, research on temporal NO_3^- fluctuations in groundwater is important for appropriate groundwater management and monitoring in addition to the investigation of horizontal and vertical nitrate fluctuation.

In Shimabara City, Nagasaki, Japan, where groundwater is a common source for drinking water supply, spatial investigations of nitrate pollution was done from 2011 to 2013 (Nakagawa et al. 2016). Nakagawa et al.

(2016) found that nitrate in this area originated from livestock waste, manure and chemical fertilizers. High NO_3^- concentrations were located in downstream of the area with high potential nitrate loading. NO_3^- concentrations fluctuation in groundwater was found to be in good agreement with rainfall events inducing wash-out and dilution. However, information on vertical NO_3^- distribution is often absent in research literature. Thus, the main objective of this study was to reveal the vertical profile of NO_3^- by using a multi-level groundwater sampler and to study processes related to rainfall events and crop systems. To understand the vertical characteristics of groundwater chemistry, hydro-geochemical components were investigated to determine factors controlling water quality.

Materials and methods

Experimental site

To monitor groundwater chemistry with soil depth, two 50 m multi-level observation wells (O-1 and O-2) were equipped at an elementary school area (31 m a.m.sl.) in Shimabara Prefecture, Nagasaki, Japan. The average groundwater table depth in the area is about 3.7 m below soil surface during March 2013 to November 2015. The average annual precipitation during 2013 to 2015 was 2,225 mm, with the highest monthly precipitation (363.5–603.5 mm) during June to August (Japan Meteorological Agency 2016). The June to August precipitation represented 38% in 2013, and over 50% in 2014 and 2015, of the annual total. The average annual temperature was 17.2°C. The rural area is mainly used of agriculture interspersed by fallow land and building (Fig. 1). Buildings are mainly located along the public road. A river flows near the observation wells. Water sampling of the river water indicate high NO_3^- level exceeding 50 mg L^{-1} (Nakagawa et al. 2016). Chinese radish, carrot, and Chinese cabbage are common crops in Shimabara. Secondary crops are lettuce, sweet corn, and watermelon.

Double cropping is performed with various crop combinations (e.g., fall/winter Chinese radish and spring carrot, winter carrot and spring carrot, then Chinese cabbage and sweat melon).

The distance between the two observation wells was 5 m (Fig. 1). Figure 2 shows a schematic of both observation wells. The 50 m deep observation wells were constituted by a 10% aperture ratio PVC screen with inner and outer diameter of 51 and 60 mm, respectively. The space between pore wall and casing pipes were filled by silica sand (ϕ 0.8-3.1 mm) to prevent breakup of pore wall and inflow of sand.

Figure 3 shows the geological profile with boring core pictures for O-1. Boring cores were composed of three kinds of matrix depending on soil depth; filling (0–1.4 m), fan deposits (1.4–44.9 m), and pyroclastic flow deposits (44.9–50.0 m). Umber cohesive soil is predominant between 0.7–0.9 m soil depth containing hard andesite gravel. The matrix between 7.1–18.5 m is rich in fine fractions, while matrix between specific depths (1.4–7.1 m and 18.5–44.9) consists of high loose and coarse sand. They include hard andesite gravel. Gravel fractions varies with depth; 60-70% (1.4–7.1 m), 30–40% (18.5–26.5 m) and 60–70% (26.5–44.9 m), respectively. Starting from a depth of 45 m, volcanic fine/medium sand is mixed with fine fractions of hard andesite gravel (50–60%).

Sampling

Figure 4 shows a schematic of sampling method. For multi-depth sampling, a Simultaneous Groundwater Extraction Apparatus (Marui & Co., Ltd.) was used. The procedure to collect water samples by this apparatus involves three steps. First, inner tubes with 11 % aperture ratio (1.06 m length) are slowly inserted into the well from the bottom and up until the entire depth is complete (50 m). Second, outer tubes, covering the inner

tubes, are inserted into the well from the top. Third, the tubes are pulled up by a chain block and separated. In order to minimize disturbance of groundwater, step 2 was done after 1 hr. Owing to this technique, undisturbed groundwater samples of about 650 mL were collected at the saturated zone; the maximum number of samples was 44.

Chemical analyses

Sampling campaigns were different for O-1 and O-2 (Table 1). This was due to the long time requirements for using Sequential Groundwater Extraction Apparatus. In March and September 2013, groundwater samplings were done at O-1. For O-2, 8 sampling campaigns were done between May 2013 to November 2015. Two of these, April 30 and August 11 2015, were conducted for each meter from 4 to 20 m and 5 to 15 m by use of a peristaltic pump. Hydrochemical parameters analyzed on site were DO, EC, pH, ORP, and HCO_3^-. Measurement of DO was performed using an HQd portable meter (HACH HQ30d). EC, pH, and ORP were measured using a handheld electrode (HORIBA D-54). HCO_3^- was quantified using titration method with 0.1 N HCl. Laboratory analyses were performed for dissolved cations (Na^+, K^+, Mg^{2+}, Ca^{2+}) and anions (Cl^-. NO_3^-, SO_4^{2-}). For analysis of these ions, groundwater samples were kept in polyethylene bottles and stored in a refrigerator before analysis using ion chromatography of suppressor type (Metrohm 861Advanced Compact IC).

Principal component analysis (PCA) is often performed on geophysical data (Aiuppa et al. 2003; Singaraja et al. 2014; Salman et al et al. 2015; Thivya et al. 2015; Zakhem and Hafez 2015; Hanssen et al. 2016; Matiatos et al. 2016) and it is a powerful tool to identify important processes (e.g., anthropogenic activities, ion exchange, weathering, mineralization, dissolution, seawater intrusion and evaporation) controlling groundwater

chemistry. Nakagawa et al. (2016) used PCA to extract importance of nitrate pollution and dissolution of ions. They showed that significance of these factors varied at each sampling location. In this study, we similarly presumed that groundwater samples from different depths are affected by different factors due to inhomogeneity of geology recharge. To confirm this hypothesis, PCA was performed for groundwater samples at different depths by the statistical software JMP Pro 11 (SAS Institute Inc.).

Results and discussion

Vertical hydrochemistry profiles

Table 1 presents a summary of descriptive statistics for major ion concentrations, DO, EC, pH, and ORP and the multi-depth sampling. Figure 5 shows the vertical profiles of hydro chemical components in the groundwater samples O-1. In March 2013, groundwater chemistry gradually changed at specific depth ranges regardless of ion type. For all ions except HCO_3^- there was a marked transition zone (27–33 m). EC values strongly reflected the dissolved ion concentrations for specific depth and ions. NO_3^- concentrations were high throughout the entire depth range although it decreased below the transition zone, indicating impacts of agricultural activities as shown by Nakagawa et al. (2016). In a study in South Korea, two distinct groundwater zones were observed due to a silty soil layer (Choi et al. 2010). However, in our study low permeable layer silt and/or clay does not appear within 50 m depth. Comparing vertical chemistry profiles with geological profiles (Fig. 3), the transition zone was observed a little deeper than a coarse layer. As shown in Fig. 3, the layer above 18.5 m depth is distinct from that below it (18.5–44.9 m) in terms of coarseness. This means that permeability is higher at the deeper layers (below 18.5 m). In other words, groundwater velocity will be faster there. Hence, one of the factors causing

a transition zone is due to different permeability of the soil layers. Thus, ion concentrations did not change abruptly but rather gradually because due to the changing velocity of groundwater. The difference between upper and lower layers seems to determine the vertical profile of ORP. Though ion concentrations and EC values decreased at the transition zone, DO values increased. pH appeared constant with depth showed weak alkalinity throughout the entire depth. The alkalinity is caused by application of lime to mitigate soil acidification for cropping (Chae et al. 2004).

In September 2013 as well as in March 2013, EC and ion components except for Na displayed a transition zone at the specific depth (Fig.5). However, while the ion concentrations increased from March below the transition zone, they increased or did not change at the shallower depth. Concentration fluctuations depending on depth are affected by factors such as recharge of precipitation from the surface (Sorensen et al. 2015). DO values showed a distinct vertical profile compared to March. The DO values at the shallow depth tend to be higher than that at the deeper depth. pH decreased to a minor extent throughout the depth and displayed a but weak alkalinity. Although ORP became lower regardless of depth, high values appeared at the specific depth (30-37 m).

Figures 6 and 7 show the vertical profiles of hydrochemical components in the groundwater samples O-2 during May 2013 and October 2014, and April 2015 to December 2015, respectively. As well as O-1, ion concentrations were changed at the specific depth as shown in Figs. 6 and 7. The transition zone, which is shallow compared to O-1, varied rather by sampling campaigns. There is no geological profile data for O-2 but the geochemical results suggest that the geology for O-1 and O-2 is similar. Higher K^+ concentrations were observed locally, indicating that these depths contain potassium feldspar which are rich in K. In addition, depths with high K^+ concentrations correspond to depths with high Cl^- concentrations. This agreement is due to application of

potassium chloride (KCl) fertilizer and manure. Ion concentrations in groundwater samples below the transition zone are often smaller than that above it. However, NO_3^-, Na^+, and Mg^{2+} concentrations increased in July 2013. Vertical profile of EC for this date is very similar to that of Na^+ and Mg^{2+}, indicating that EC is controlled by Na^+ and Mg^{2+}. Except for the drastic change in July 2013, the general trend is increasing DO with depth also at O-2. pH showed weak alkalinity as well at O-2 and varied to weak acidity. The ORP varied widely by the sampling campaign but showed oxic condition throughout the entire depth.

Agricultural and precipitation impacts

As shown in Figs. 5, 6, and 7, NO_3^- concentrations were high throughout all depths. This means agricultural activities affect groundwater recharge area. Temporal fluctuation of NO_3^- concentration in groundwater is modified by many processes from application of fertilizer to arrival to the groundwater. Crops with deep roots can absorb more NO_3^- and balance leaching to the groundwater better as compared to crops with short roots (Kundu et al. 2009). However, in case of intensive irrigation crops develop short roots meaning that they have smaller uptake ability of water and nutrients. Thus, downward movement of NO_3^- is promoted that results in high NO_3^- concentrations below the root zone (Dahan et al. 2014). In the soil matrix, upward and downward NO_3^- migration is controlled by soil moisture that in turn is affected by evaporation, rainfall, and irrigation amounts (Huang et al. 2013). NO_3^- accumulation in soil and soil water was observed at the specific depth after the crop season and its peak concentrations significantly depended on N application rate (Li et al. 2016). Thus, although NO_3^- concentration in the shallow groundwater has similar temporal trend with leachate concentration, there is a lag time between them (Derby et al. 2007). N fertilizer surplus will pass through the crop

root zone and move towards the groundwater surface under the influence of various hydrological processes. Precipitation events affect not only NO_3^- concentration (Sorensen et al. 2015) but also water chemistry (Padilla et al. 2015) of soil water and groundwater. In our study, temporal NO_3^- concentration was closely correlated with daily precipitation and cultivation system (Fig. 8). As mentioned above, concentration fluctuation depends on the soil depth so that NO_3^- concentrations were averaged by distinguishing the depth (above 18 m and below 30 m depth). In Shimabara City, large areas are used for cultivation of radish, carrot, and Chinese cabbage. Some areas are used for lettuce and water melon. Yield amounts for lettuce and watermelon represent 10-25% as compared to the predominant crops (radish, carrot, and Chinese cabbage). Figure 8 shows typical annual cultivation systems for these crops. For example, in the case of double cropping of radish and carrot, seeding is performed between August and September. They are harvested between November and December. Subsequently, seeding is again conducted in December with harvest in April. Not all crops are harvested. A part is left in the cultivation to use them as green manure. In the case of lettuce, seeding is in August and December. It is harvested in October-December. Cropping of watermelon is followed by Chinese cabbage. Manure is commonly applied as soil amendment before first cropping. Basic fertilizers are utilized before first and second cropping. The variation of NO_3^- concentration at O-1, decreased at shallow depths and increased at deeper depth on September 6, 2013. NO_3^- concentration was diluted shallow depth due to recharge from abundant precipitation (570 mm from August 23 to September 4 in 2013). The sampling campaign started soon after seeding, which means that nitrogen uptake by crops was less. Thus, large amounts of precipitation promoted leaching and downward migration of nitrogen components in recharge. Therefore, NO_3^- concentration was elevated at larger depths. However, concentration fluctuation was small, which suggests that nitrate mass had already passed through or not reached observation

points. Secondly, when the variation of NO_3^- concentration for O-2 was observed carefully, NO_3^- concentration showed discriminative change in July 2, 2013. It is because that NO_3^- concentration decreased significantly at the shallow depth, and the magnitude relation between concentrations at the shallow and deep depth was reversed. In other words, the NO_3^- concentration at the deep depth became higher than that at the shallow depth. This relationship was observed on only July 2, 2013 through the entire sampling campaign. The decrease can be a result of dilution by precipitation recharge. It more or less rained continuously from June 15 to July 1 2013 (in total 233.5 mm). Although the amount of rainfall is one of the around two compared to the case of O-1, the extent of decrease in concentration is larger, suggesting relationship between temporal fluctuation of NO_3^- concentration and cultivation system just as same. Although O-1 was affected practically by reaching of accumulated NO_3^- at the same time while the dilution effect occurred, O-2 was affected by not reaching of NO_3^- but only dilution. Hence, two-fold reduction of concentration occurred at O-2. In next sampling campaign (September 6, 2013), the magnitude relation between concentrations at the shallow and deep depth got back, which means that NO_3^- concentration at the shallow depth is higher than that at the deep depth. After that, NO_3^- concentration was stable and the discriminative variation of it was not observed before August 11, 2013. In this date, NO_3^- concentration at the shallow and deep depth decreased simultaneously. Although it was no rain from July 29 to August 11, that was not caused by dilution like last decline. This result suggest that the amount of NO_3^-, which pass though the root zone and is accumulated, decreases because of rainfall and fertilization timings.

On November 26, 2015, the highest NO_3^- concentrations throughout the entire sampling campaign both at shallow and larger depths appeared. This indicated that accumulated NO_3^- mass in the soil reached the groundwater. However, we can not decipher when this nitrate was applied and how long it had been accumulated .

This means that additional time series data such as temporal NO_3^- concentration in the soil and soil water from multi-depth in unsaturated zone will be required.

Principal component analysis

Principal component analysis (PCA) was applied by using correlation coefficient matrix based on a subset of selected hydrochemical parameters (Cl^-, NO_3^-, SO_4^{2-}, HCO_3^-, Na^+, K^+, Mg^{2+}, and Ca^{2+}) to identify the factors regulating vertical groundwater chemistry. The number of principal components (PC) was determined with Kiser criteria which takes into account only factors having eigenvalues larger than 1.0. Table 2 shows the obtained result of PCA as mentioned above procedure. Three PCs were extracted that explained 83% of the total variance.

Factor 1, representing the highest variance (46 %), was characterized by high and moderate loadings for all major ions (Cl^-, NO_3^-, SO_4^{2-}, HCO_3^-, Na^+, K^+, Mg^{2+}, and Ca^{2+}), indicating that groundwater evolved from various processes. The correlation with Cl^-, NO_3^-, SO_4^{2-}, and K^+ represent the infiltration of chemical fertilizer and manure applied in agricultural field according to Nakagawa et al. (2016). Apart from nitrogen, chemical fertilizer which contains Mg and Ca is often used because these element are also essential for crops. Hence, application of chemical fertilizer can contribute to increase of specific ions. The positive loadings of HCO_3^-, Na^+, K^+, Mg^{2+}, and Ca^{2+} are also associated with weathering of minerals such as feldspar, calcite and dolomite by water-rock interaction during groundwater flows. Thus, Factor 1 can be interpreted as the amount of dissolved ions containing the influence of anthropogenic and natural impacts. The positive loadings of NO_3^- and Na^+ then the negative loading of SO_4^- and HCO_3^- are revealed by Factor 2 accounting for 23% of the total variance. The positive loading of NO_3^- indicates the impacts of N-fertilizer. However, because SO_4^{2-} shows a negative loading, NO_3^- of

Factor 2 can not originate from ammonium sulfate $(NH_4)_2SO_4$ but instead ammonium nitrate NH_4NO_3. The dissolution of Na-silicate mineral such as albite is represented by the positive loading of Na^+. Thus, Ca^{2+} shows small but negative correlation, indicating that cation exchange may occur between Na^+ and Ca^{2+} (Singaraja et al. 2014). Factor 3 was positively correlated with Cl^- and K^+, representing 14% of the total variance. This factor indicates the input of agricultural fertilizer such as potassium chloride (KCl) and dissolution of orthoclase. In addition, cation exchange is also inferred by the positive K^+ loading and the weak negative Mg^{2+} and Ca^{2+} loadings (Singaraja et al. 2014). Factor 1 contains the same meaning as Factor 2 (influence of ammonium sulfate and dissolution of albite) and Factor 3 (impact of potassium chloride and dissolution of orthoclase) because Factor 1 shows positive values for all ions. Hence, the influence of them can be distinguished by Factor 2 and 3.

Principal component (PC) / Factor scores are used to distinguish the spatial trends of hydrochemical processes (Aiuppa et al. 2003; Singaraja et al. 2014; Matiatos et al. 2016). In this study, we attempted to understand the difference impacts by soil depth by plotting PC scores vs depth. The three vertical PCs variation is described by each sampling campaign in Fig. 9. Principal component scores of Factor 1 which represent the amount of dissolved ion concentration varied from -2.96 to 5.20 and changed gradually from the specific depths. As a matter of fact this vertical variation is similar with that of ions and EC as shown in Figs. 5, 6, and 7.

The vertical variation of Factor 2 scores represented by influence of ammonium nitrate (NH_4NO_3) and dissolution of albite is in between -4.99 and 3.11, showing discriminative change on July 2, 2013 and November 26, 2015. As mentioned above, dilution of NO_3^- was caused by high amount of precipitation on July 2, 2013. The accumulated NO_3^- mass reached the groundwater on November 26, 2015. The variation of Factor 2 scores is in good agreement with vertical change of NO_3^- for these sampling campaigns (Figs. 6, 7 and 9), indicating that NO_3^-

originated from NH_4NO_3 occupying large part of subsistent NO_3^- in these periods. Except for these sampling data, Factor 2 scores fall in between -1.70 and 1.62. The vertical profile of them is almost uniform and does not change much. However, the magnitude relation of PC scores between Factor 1 and 2 is reversed because that of Factor 1 decrease at the specific depths. In other words, that of Factor 2 are predominant below the transition zone compared to Factor 1, which is caused by the differences of application rate of NH_4NO_3 fertilizer at the recharge area of groundwater and the plentiful occurrence of albite.

PCs of Factor 3 means impact of potassium chloride (KCl) and dissolution of orthoclase ranged from -1.46 to 8.40. At the specific depth with high scores, larger amount of orthoclase can exist within the deposits. As well as PC scores of Factor 2, the magnitude relation of PC scores between Factor 1 and 3 is reversed, also indicating differences of the usage rate of KCl fertilizer at the recharge area of groundwater and the plenty of orthoclase. Further, cation exchange may occur due to predominance of Factor 2 and 3 below the transition zone.

Conclusion

In this study, groundwater samples collected from different soil depths to assess vertical groundwater characteristic including nitrate pollution at an intensive agricultural area. For both observation wells, the transition zone appeared for all ions at a specific depth. This is due to different groundwater velocity caused by distinct deposit coarseness because low permeable and/or impermeable layers such as silt and clay layers are absent in core samples. Although NO_3^- concentration declined from the transition zone, it still exceeded permissible level (50 mg L^{-1}) for drinking determined by WHO. The temporal decline of NO_3^- concentration was significantly affected by high amount of precipitation recharge at the shallow depth. Accumulated NO_3^- in the soil resulted in

increase of NO_3^- concentration. However, we need additional data to assess NO_3^- migration exactly in the soil matrix until it passes through crops roots zone and is infiltrated within groundwater. PCA brings out anthropogenic impacts (application of manure and fertilizer as ($(NH_4)_2SO_4$, NH_4NO_3, and KCl), dissolution minerals, and ion exchange as the factors regulating groundwater chemistry, then principal components score revealed that NH_4NO_3 and KCl fertilizers was applied dominantly in the groundwater recharge area at larger depth when containing albite and orthoclase larger.

For future research, we will investigate different recharge zone by examining environmental isotopic data ($\delta^{18}O$ andδ^2H of H_2O), which is utilized commonly, from multi-level groundwater samples. Then, NO_3^- migration (time lag from application of fertilizer to reaching) in the soil matrix at the recharge area will be understand by investigating temporal soil NO_3^- and soil water NO_3^- content in the unsaturated zone. From these study, different fluctuation of NO_3^- content by the depth will be revealed. The long-term field research is required to understand NO_3^- fate completely, which means that important NO_3^- fluctuation in the soil and groundwater might be missed if the study is conducted in short-term (Derby et al. 2009), so that observation of multi-level groundwater should be continued with advanced research.

Acknowledgements

This work was supported by JSPS KAKENHI Grant Number 24360194 and 15KT0120.

References

Ağca N, Karanlık S, Ödemiş B (2014) Assessment of ammonium, nitrate, phosphate, and heavy metal pollution in groundwater from Amik Plain, southern Turkey. Environ Monit Assess 186(9):5921-5934. doi:10.1007/s10661-014-3829-z

Aiuppa A, Bellomo S, Brusca L, D'Alessandro W, Federico C (2003) Natural and anthropogenic factors affecting groundwaterquality of an active volcano (Mt. Etna, Italy). Applied Geochemistry 18(6):863-882. doi:10.1016/S0883-2927(02)00182-8

Chandna P, Khurana ML, Ladha JK, Punia M, Melha RS, Gupta R (2011) Spatial and seasonal distribution of nitrate-N in groundwater beneath the rice–wheat cropping system of India: a geospatial analysis. Environ Monit Assess 178(1):545-562. doi:10.1007/s10661-010-1712-0

Choi BY, Yun ST, Mayer B, Chae GT, Kim KH, Kim K, Koh YK (2010) Identification of groundwater recharge sources and processes in a heterogeneous alluvial aquifer: results from multi-level monitoring of hydrochemistry and environmental isotopes in a riverside agricultural area in Korea. Hydrol Process 24(3):317-330. doi: 10.1002/hyp.7488

Dahan O, Babad A, Lazarovitch N, Russak EE, Kurtzman D (2014) Nitrate leaching from intensive organic farms to groundwater. Hydrol Earth Syst Sci 18(1):333-341. doi:10.5194/hess-18-333-2014

Derby NE, Casey FXM, Knighton RE (2009) Long-term observation of vadose zone and groundwater nitrate concentrations under irrigated agriculture. Vadose Zone J 8(2):290-300. doi:10.2136/vzj2007.0162

Esmaeili A, Moore F, Keshavarzi B (2014) Nitrate contamination in irrigation groundwater, Isfahan, Iran. Environ Earth Sci 72(7): 2511-2522. doi:10.1007/s12665-014-3159-z

Hassen I, Hamzaoui-Azaza F, Bouhlila R (2016) Application of multivariate statistical analysis and hydrochemical and isotopic investigations for evaluation of groundwater quality and its suitability for drinking and agriculture purposes: case of Oum Ali-Thelepte aquifer, central Tunisia. Environ Monit Assess 188(3):135. doi:10.1007/s10661-016-5124-7

Huang T, Pang Z, Yuan L (2013) Nitrate in groundwater and the unsaturated zone in (semi)arid northern China: baseline and factors controlling its transport and fate. Environ Earth Sci 70(1):145-156. doi:10.1007/s12665-012-2111-3

Jalali M (2011) Nitrate pollution of groundwater in Toyserkan, western Iran. Environ Earth Sci 62(5): 907-913. doi:10.1007/s12665-010-0576-5

Japan Meteorological Agency (2015) Weather observation data. Japan Meteorological Agency Web, http://www.jma.go.jp/jma/index.html (Accessed 5 February 2016)

Ju XT, Kou CL, Zhang FS, Christie P (2006) Nitrogen balance and groundwater nitrate contamination: Comparison among three intensive cropping system on the North China Plain. Environ Pollut 143(1):117-125. doi:10.1016/j.envpol.2005.11.005

Ki MG, Koh DC, Yoon H, Kim H (2015) Temporal variability of nitrate concentration in groundwater affected by intensive agricultural activities in a rural area of Hongseong, South Korea. Environ Earth Sci 74(7): 6147-6161. doi:10.1007/s12665-015-4637-7

Kundu MC, Mandal B, Hazra GC (2009) Nitrate and fluoride contamination in groundwater of an intensively managed agroecosystem: A functional relationship. Sci Total Environ 407(8):2771-2782. doi:10.1016/j.scitotenv.2008.12.048

Li Y, Liu H, Huang G, Zhang R, Yang H (2016) Nitrate nitrogen accumulation and leaching pattern at a winter wheat: summer maize cropping field in the North China Plain. Environ Earth Sci 75:118. doi:10.1007/s12665-015-4867-8

Liu GD, Wu WL, Zhang J (2005) Regional differentiation of non-point source pollution of agriculture-derived nitrate nitrogen in groundwater in northern China. Agric Ecosyst Environ 107(2-3):211-220. doi:10.1016/j.agee.2004.11.010

Matiatos I (2016) Nitrate source identification in groundwater of multiple land-use areas by combining isotopes and multivariate statistical analysis: A case study of Asopos basin (Central Greece). Sci Total Environ 541:802-814. doi:10.1016/j.scitotenv.2015.09.134

Nakagawa K, Amano H, Asakura H, Berndtsson R (2016) Spatial trends of nitrate pollution and groundwater chemistry in Shimabara, Nagasaki, Japan. Environ Earth Sci 75:234. doi: 10.1007/s12665-015-4971-9

Nemčić-Jurec J, Konjačić M, Jazbec A (2013) Monitoring of nitrates in drinking water from agricultural and residential areas of Podravina and Prigorje (Croatia). Environ Monit Assess 185(11):9509-9520. doi:10.1007/s10661-013-3269-1

Padilla C, Onda Y, Iida T (2015) Interaction between runoff–bedrock groundwater in a steep headwater catchment underlain by sedimentary bedrock fractured by gravitational deformation. Hydrol Process 29(20): 4398–4412. doi:10.1002/hyp.10498

Salman AS, Zaidi FK, Hussein MT(2015) Evaluation of groundwater quality in northern Saudi Arabia using multivariate analysis and stochastic statistics. Environ Earth Sci 74(12):7769-7782. doi:10.1007/s12665-014-3803-7

Singaraja C, Chidambaram S, Prasanna MV, Thivya C, Thilagavathi R (2014) Statistical analysis of the hydrogeochemical evolution of groundwater in hard rock coastal aquifers of Thoothukudi district in Tamil Nadu, India. Environ Earth Sci 71(1):451-464. doi:10.1007/s12665-013-2453-5

Sorensen JPR, Butcher AS, Stuart ME, Townsend B R (2015) Nitrate fluctuation at the water table: implications for recharge processes and solute transport in the Chalk aquifer. Hydrol Process 29(15):3355-3367. doi: 10.1002/hyp.10447

Thivya C, Chidambaram S, Thilagavathi R, Prasanna MV, Singaraja C, Adithya VS, Nepolian M (2015) A multivariate statistical approach to identify the spatio-temporal variation of geochemical process in a hard rock aquifer. Environ Monit Assess 187:552. doi:10.1007/s10661-015-4738-5

WHO (World Health Organization) (2011) Guidelines for drinking water quality, 4th edn

Zakhem BA, Hafez R (2015) Hydrochemical, isotopic and statistical characteristics of groundwater nitrate pollution in Damascus Oasis (Syria). Environ Earth Sci 74(4): 2781-2797. doi:10.1007/s12665-015-4258-1

Figure Captions

Fig. 1 Study sites and elevation

Fig. 2 Schematic of observation well

Fig. 3 Geological profiles and core pictures for observation well at O-1

Fig. 4 Schematic of sampling method

Fig. 5 Hydrochemical profiles with soil depth for groundwater at O-1. Vertical bars denote length of sampling tubes.

Fig. 6 Hydrochemical profiles with soil depth for groundwater at O-2 between May 2013 and October 2014. Vertical bars denote length of sampling tubes.

Fig. 7 Hydrochemical profiles with soil depth for groundwater at O-2 between April and November 2015. Vertical bars denote length of sampling tubes. P-denoted sampling was done by peristaltic pump.

Fig. 8 Daily precipitation, cropping system, and temporal variation of mean NO_3^- concentration above 18 m and below 30 m soil depth between January 1 2013 and December 30 2015.

Fig. 9 Vertical variation of principal component scores. The figures of first row represent results of O-1. The second row and subsequent figures represent results of O-2.

Table captions

Table 1 Descriptive statistics of major ion concentrations, DO, EC, pH, and ORP from multi-level samples

Table 2 Principal component analysis of major ion concentrations

Table 1 Descriptive statistics of major ion concentrations, DO, EC, pH, and ORP from multi-level samples

Site	Date	Method		Cl^-	NO_3^-	SO_4^{2-}	HCO_3^-	Na^+	K^+	Mg^{2+}	Ca^{2+}	DO	EC	pH	ORP
				mg L^{-1}	mg L^{-1}	mg L^{-1}	mg L^{-1}	mg L^{-1}	mg L^{-1}	mg L^{-1}	mg L^{-1}	mg L^{-1}	mS m^{-1}		mV
O-1	3/14/13	SGEA	Max	43.5	94.4	38.7	43.9	20.0	27.5	12.9	41.8	9.2	60.6	7.67	386
			Min	15.6	57.5	15.8	20.5	14.1	6.8	7.6	21.1	7.5	30.8	6.80	214
			Mean	22.1	80.6	25.5	30.5	16.8	8.9	10.4	30.8	8.6	40.3	7.36	262
			SD	4.9	10.7	7.5	7.3	1.9	3.1	2.1	6.9	0.6	7.9	0.16	45
O-1	9/6/13	SGEA	Max	33.2	89.4	35.8	42.9	19.5	15.1	13.1	39.9	9.5	48.9	7.62	257
			Min	18.9	68.7	19.4	23.3	15.2	6.6	8.4	23.5	5.8	32.8	6.99	122
			Mean	24.1	77.2	28.6	33.2	16.8	8.6	10.4	32.8	8.1	42.1	7.26	167
			SD	3.6	5.3	5.9	5.6	1.0	1.6	1.3	5.3	0.7	4.6	0.16	27
O-2	5/30/13	SGEA	Max	32.3	88.7	33.5	57.9	19.1	16.4	12.5	44.5	9.1	61.7	7.89	283
			Min	16.5	63.6	10.9	24.4	13.4	5.9	7.5	23.0	8.1	31.4	7.39	135

			Mean	21.3	75.1	21.5	36.0	15.6	8.9	9.4	30.5	8.8	38.6	7.62	240
			SD	4.3	8.7	7.6	12.9	1.8	2.8	1.9	8.2	0.4	8.2	0.18	45
O-2	7/2/13	SGEA	Max	49.2	78.0	35.9	75.7	14.9	34.7	11.0	46.7	11.8	55.5	8.10	-
			Min	17.2	49.6	16.1	22.0	9.1	5.2	5.8	18.1	7.9	22.7	7.39	-
			Mean	23.1	69.0	25.1	46.5	13.4	9.2	8.7	33.5	10.6	41.7	7.72	-
			SD	6.3	6.2	7.6	18.5	1.6	5.3	1.3	8.7	1.2	7.2	0.21	-
O-2	11/14/13	SGEA	Max	27.1	90.0	30.9	42.4	16.7	13.2	12.0	40.8	9.4	48.3	7.69	318
			Min	17.7	64.8	16.5	18.3	9.5	6.4	7.7	22.4	7.8	31.0	7.07	103
			Mean	20.8	73.9	20.9	25.3	12.1	7.8	9.1	27.8	8.9	36.4	7.21	191
			SD	2.7	7.0	5.5	5.4	2.6	1.4	1.5	6.2	0.3	5.3	0.16	84
O-2	10/28/14	SGEA	Max	38.7	87.0	31.0	47.3	17.2	24.2	13.0	42.7	9.7	50.2	7.10	285
			Min	17.8	70.4	16.1	20.7	12.2	7.8	3.7	23.4	7.8	25.2	6.70	150
			Mean	21.6	76.6	21.5	27.6	14.4	11.0	9.7	28.8	9.1	32.0	6.94	208

			SD	4.5	6.1	5.4	6.1	1.2	3.4	2.1	5.8	0.6	6.1	0.11	34
O-2	4/23/15	SGEA	Max	28.9	103.2	33.0	34.4	16.0	13.8	14.5	45.2	9.3	31.8	7.55	269
			Min	19.0	80.8	14.7	16.5	6.8	6.5	8.8	19.7	8.4	21.8	7.22	254
			Mean	22.2	87.4	19.9	23.5	11.8	8.8	10.8	31.2	9.0	25.2	7.37	262
			SD	2.9	7.7	6.3	6.2	1.6	1.7	1.9	7.9	0.3	3.4	0.06	4
O-2	4/30/15	P	Max	23.1	97.6	28.5	31.2	15.0	10.0	13.2	38.5	8.3	44.5	6.96	279
			Min	17.2	73.3	17.6	22.8	11.2	7.8	8.3	30.2	7.7	24.6	6.72	213
			Mean	20.1	86.0	22.5	26.3	12.4	8.9	11.6	34.5	8.0	31.2	6.83	244
			SD	1.9	7.4	3.8	2.5	1.0	0.5	1.3	2.5	0.2	4.7	0.07	22
O-2	8/11/15	SGEA&P	Max	36.6	83.2	28.5	31.7	22.7	22.2	13.0	31.2	9.0	42.5	7.32	258
			Min	16.1	54.8	14.6	19.3	10.7	5.8	8.9	19.3	6.3	27.8	6.75	169
			Mean	24.1	71.5	21.8	25.5	19.1	12.0	10.8	26.5	8.0	32.6	6.90	203
			SD	4.7	6.6	5.2	3.1	2.3	4.5	1.3	2.7	0.8	3.3	0.10	20

O-2	11/26/15	SGEA	Max	33.7	126.7	30.6	35.7	24.3	11.9	13.4	40.4	9.9	37.8	7.11	184
			Min	17.8	79.5	13.2	19.6	10.8	5.4	7.2	19.9	8.8	26.6	6.88	102
			Mean	26.5	106.6	19.9	25.5	17.7	8.0	10.3	30.2	9.4	30.6	6.96	161
			SD	3.7	12.4	4.9	4.9	3.8	1.3	1.7	5.8	0.3	3.7	0.04	19

SGEA; Simultaneous Groundwater Extraction Apparatus, P; Pump, -; No data

Table 2 Principal component analysis of major ion concentrations

	Components		
	Factor1	Factor2	Factor3
Cl^-	0.82	0.17	0.40
NO_3^-	0.50	0.64	-0.37
SO_4^{2-}	0.51	-0.76	-0.08
HCO_3^-	0.68	-0.62	-0.13
Na^+	0.56	0.52	0.05
K^+	0.52	0.01	0.82
Mg^{2+}	0.80	0.31	-0.23
Ca^{2+}	0.89	-0.21	-0.31
Eigenvalues	3.66	1.81	1.13
Explained variance (%)	45.7	22.7	14.2
Cumulative explained variance (%)	45.7	68.4	82.6

Figure 1

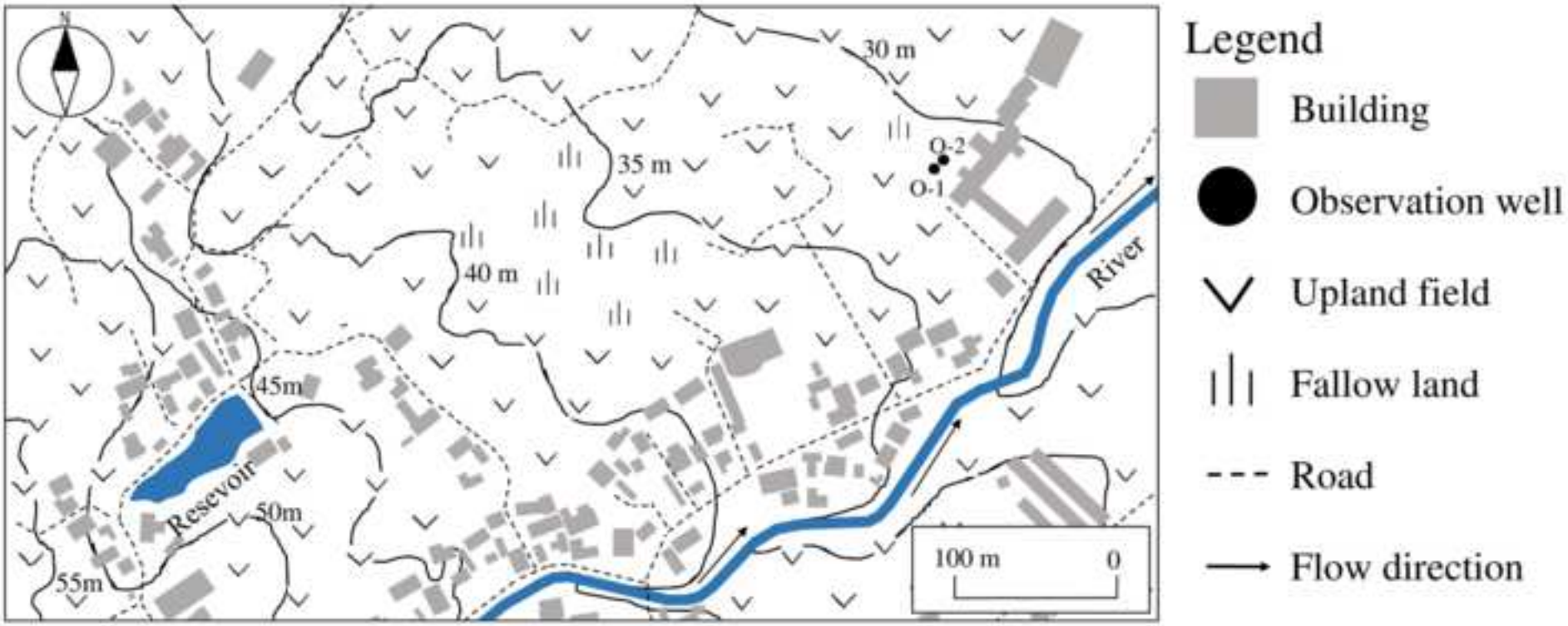
N
30 m
35 m
40 m
45m
50m
55m
O-2
O-1
Resevoir
River
100 m
0
Legend
Building
Observation well
Upland field
Fallow land
Road
Flow direction

Figure 2

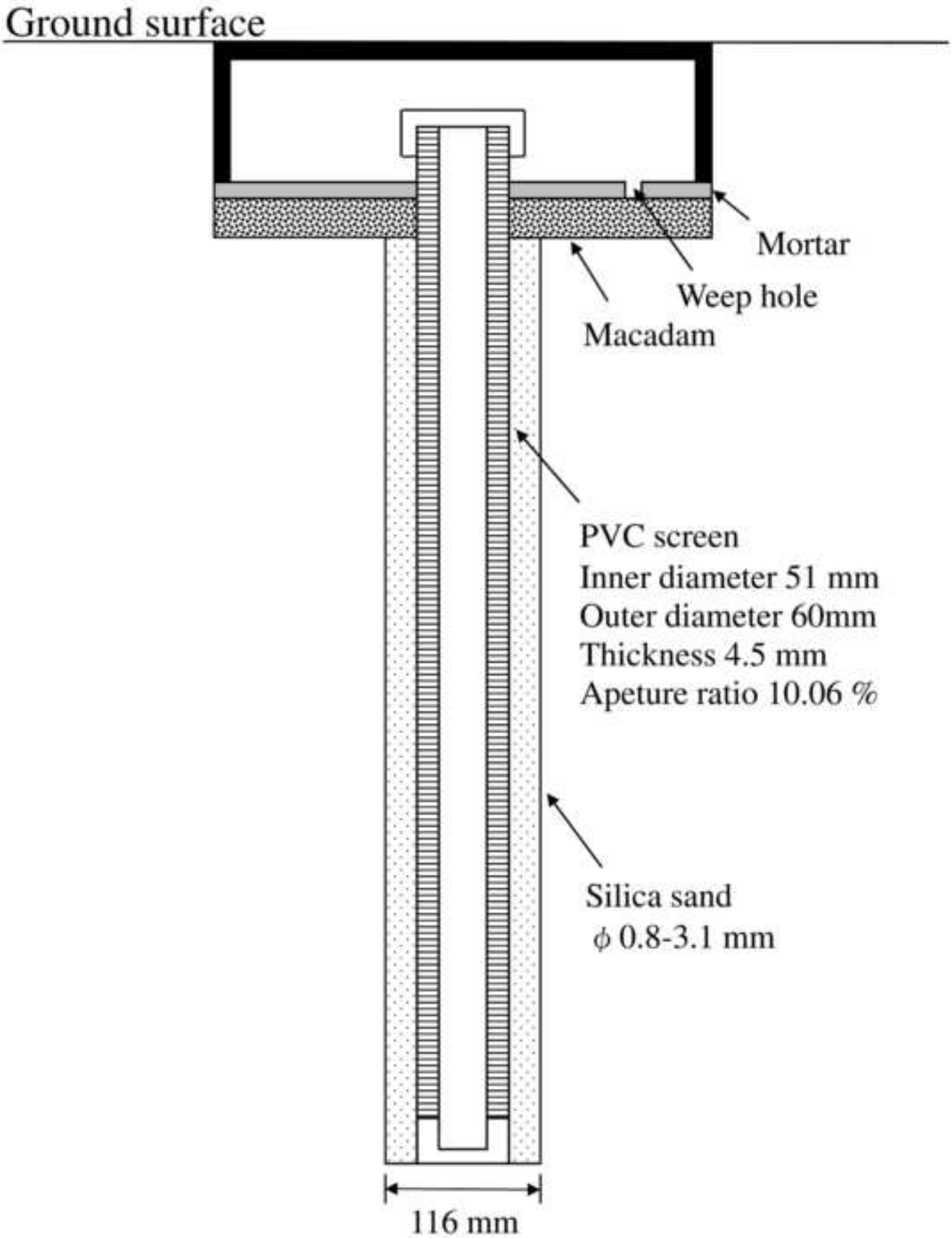
Ground surface
Mortar
Weep hole
Macadam
PVC screen
Inner diameter 51 mm
Outer diameter 60mm
Thickness 4.5 mm
Apeture ratio 10.06 %
Silica sand
ϕ 0.8-3.1 mm
116 mm

Figure 3

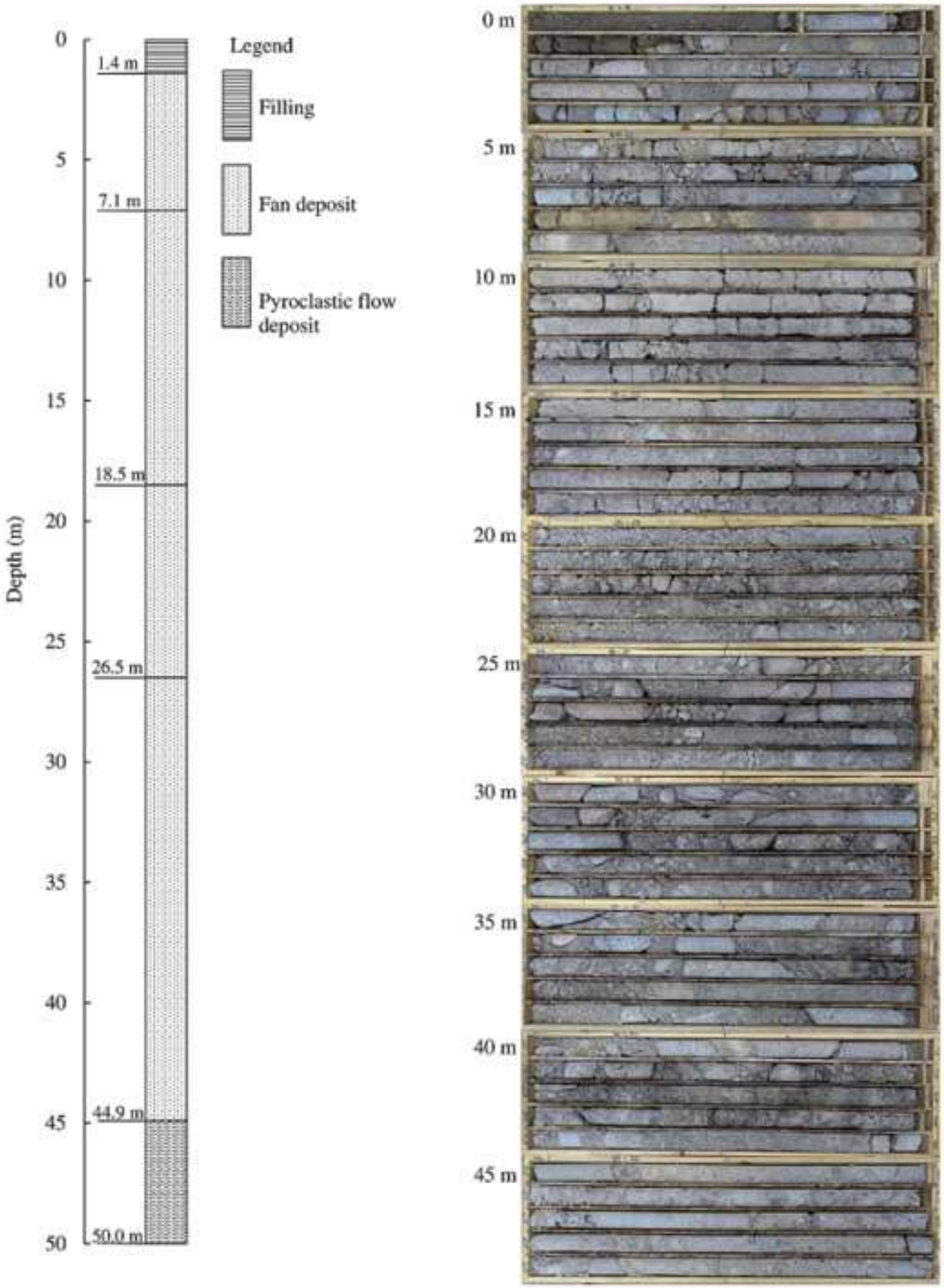
Depth (m)
0
5
10
15
20
25
30
35
40
45
50
1.4 m
7.1 m
18.5 m
26.5 m
44.9 m
50.0 m
Legend
Filling
Fan deposit
Pyroclastic flow deposit
0 m
5 m
10 m
15 m
20 m
25 m
30 m
35 m
40 m
45 m

Figure 4

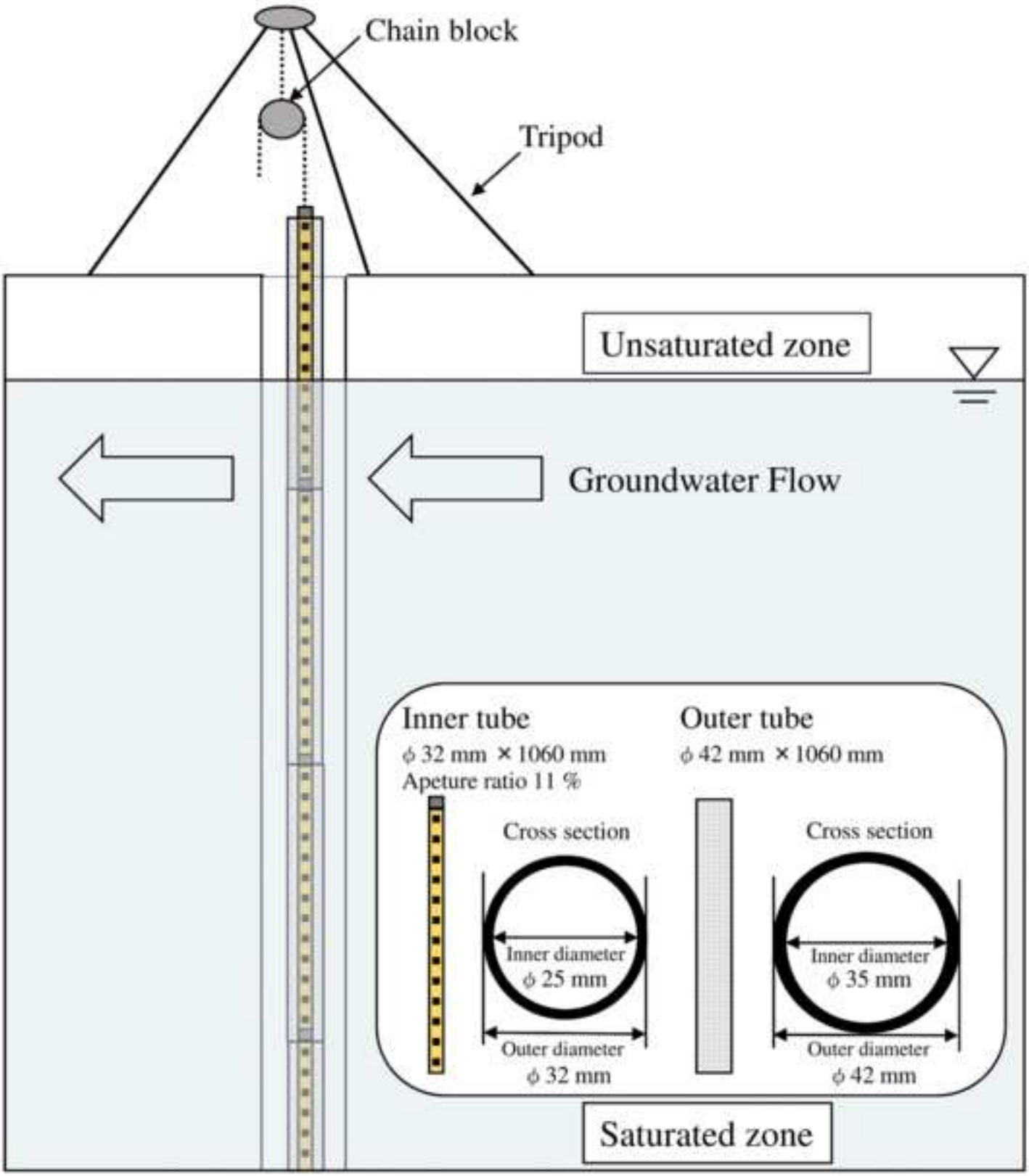
Chain block
Tripod
Unsaturated zone
Groundwater Flow
Inner tube
ϕ 32 mm × 1060 mm
Apeture ratio 11 %
Cross section
Inner diameter
ϕ 25 mm
Outer diameter
ϕ 32 mm
Outer tube
ϕ 42 mm × 1060 mm
Cross section
Inner diameter
ϕ 35 mm
Outer diameter
ϕ 42 mm
Saturated zone

Figure 5

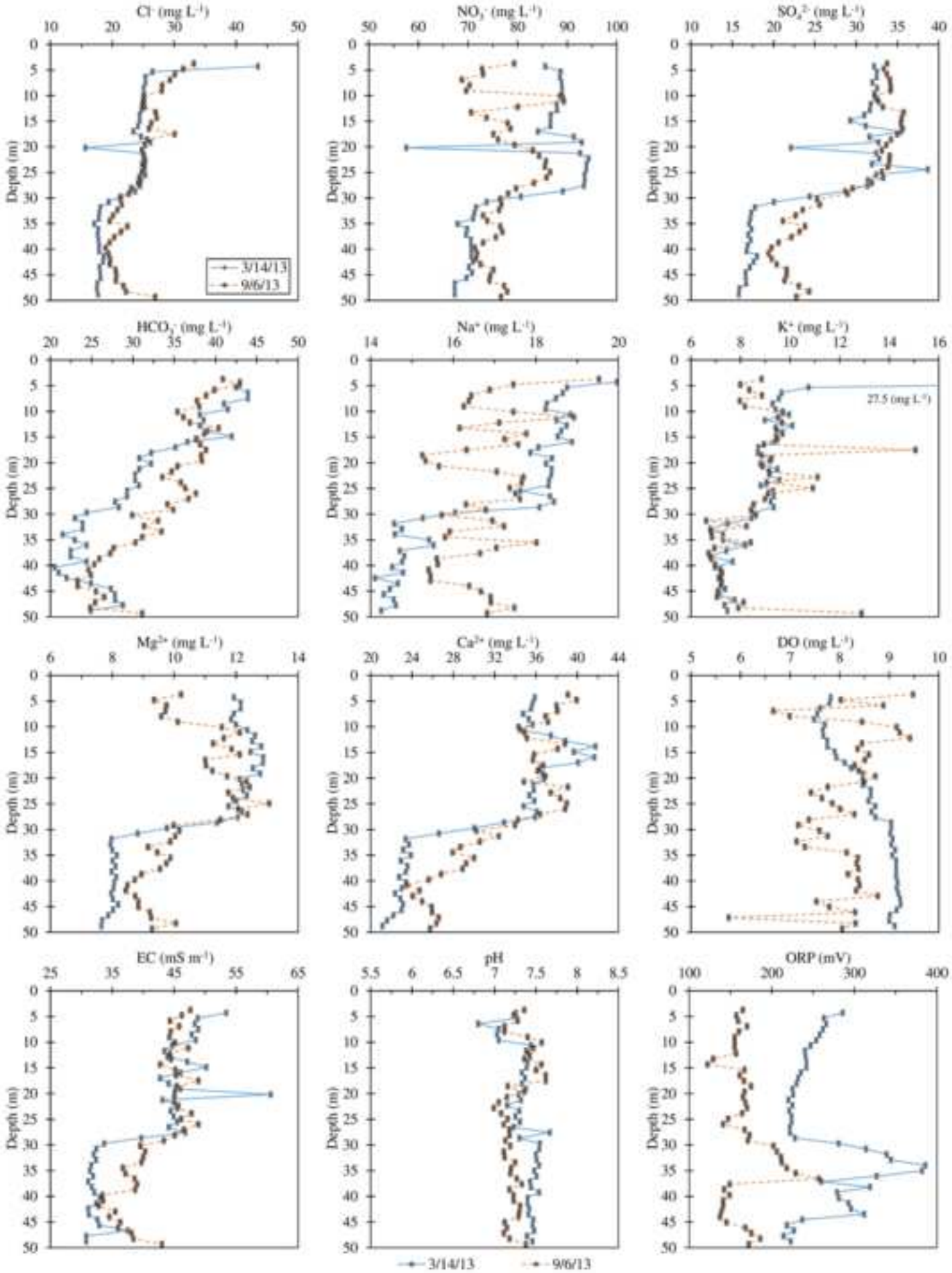
Cl⁻ (mg L⁻¹)
NO₃⁻ (mg L⁻¹)
SO₄²⁻ (mg L⁻¹)
HCO₃⁻ (mg L⁻¹)
Na⁺ (mg L⁻¹)
K⁺ (mg L⁻¹)
27.5 (mg L⁻¹)
Mg²⁺ (mg L⁻¹)
Ca²⁺ (mg L⁻¹)
DO (mg L⁻¹)
EC (mS m⁻¹)
pH
ORP (mV)
Depth (m)
3/14/13
9/6/13

Figure 6

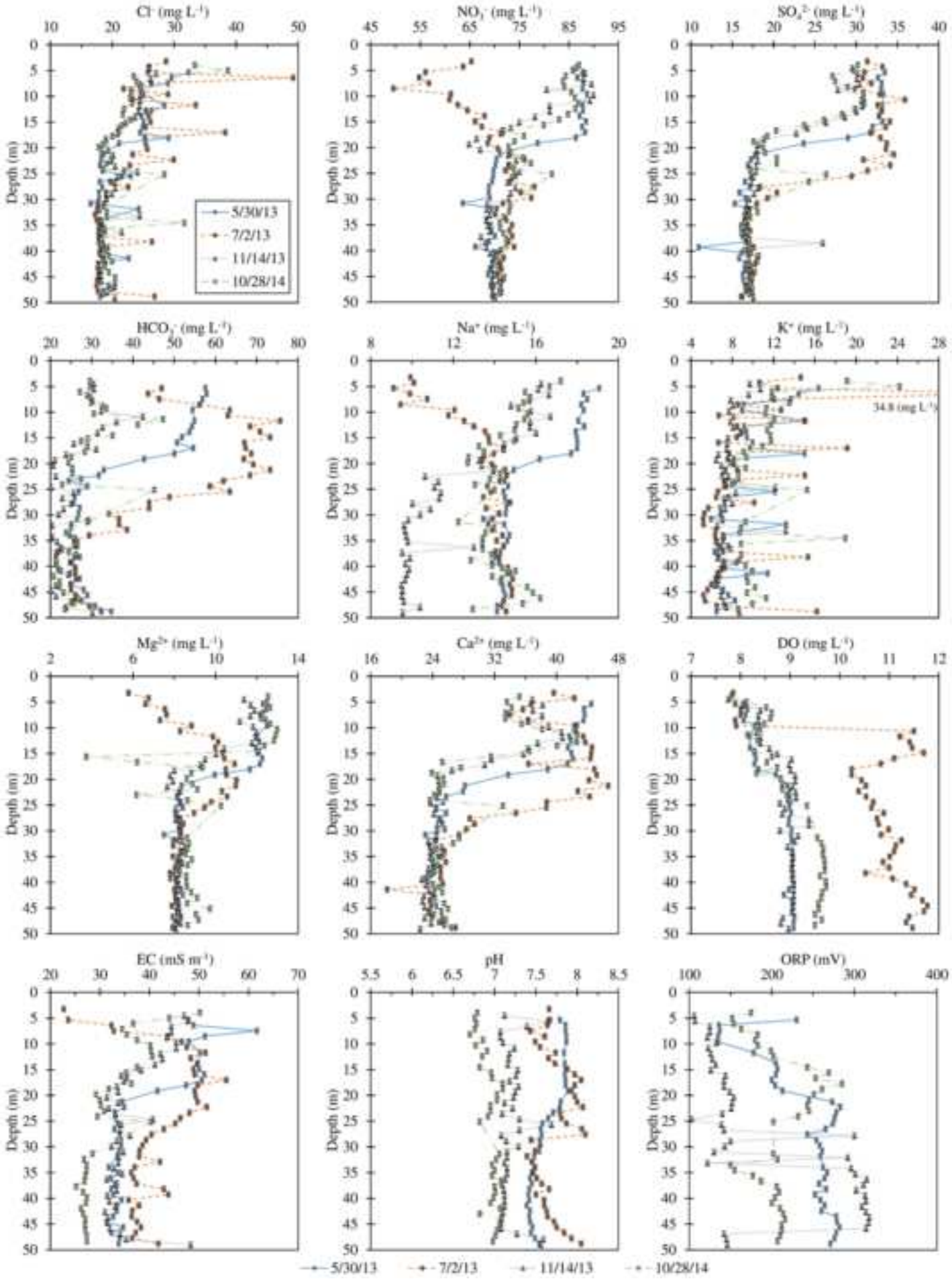
Cl⁻ (mg L⁻¹)
NO₃⁻ (mg L⁻¹)
SO₄²⁻ (mg L⁻¹)
HCO₃⁻ (mg L⁻¹)
Na⁺ (mg L⁻¹)
K⁺ (mg L⁻¹)
34.8 (mg L⁻¹)
Mg²⁺ (mg L⁻¹)
Ca²⁺ (mg L⁻¹)
DO (mg L⁻¹)
EC (mS m⁻¹)
pH
ORP (mV)
Depth (m)
5/30/13
7/2/13
11/14/13
10/28/14

Figure 7

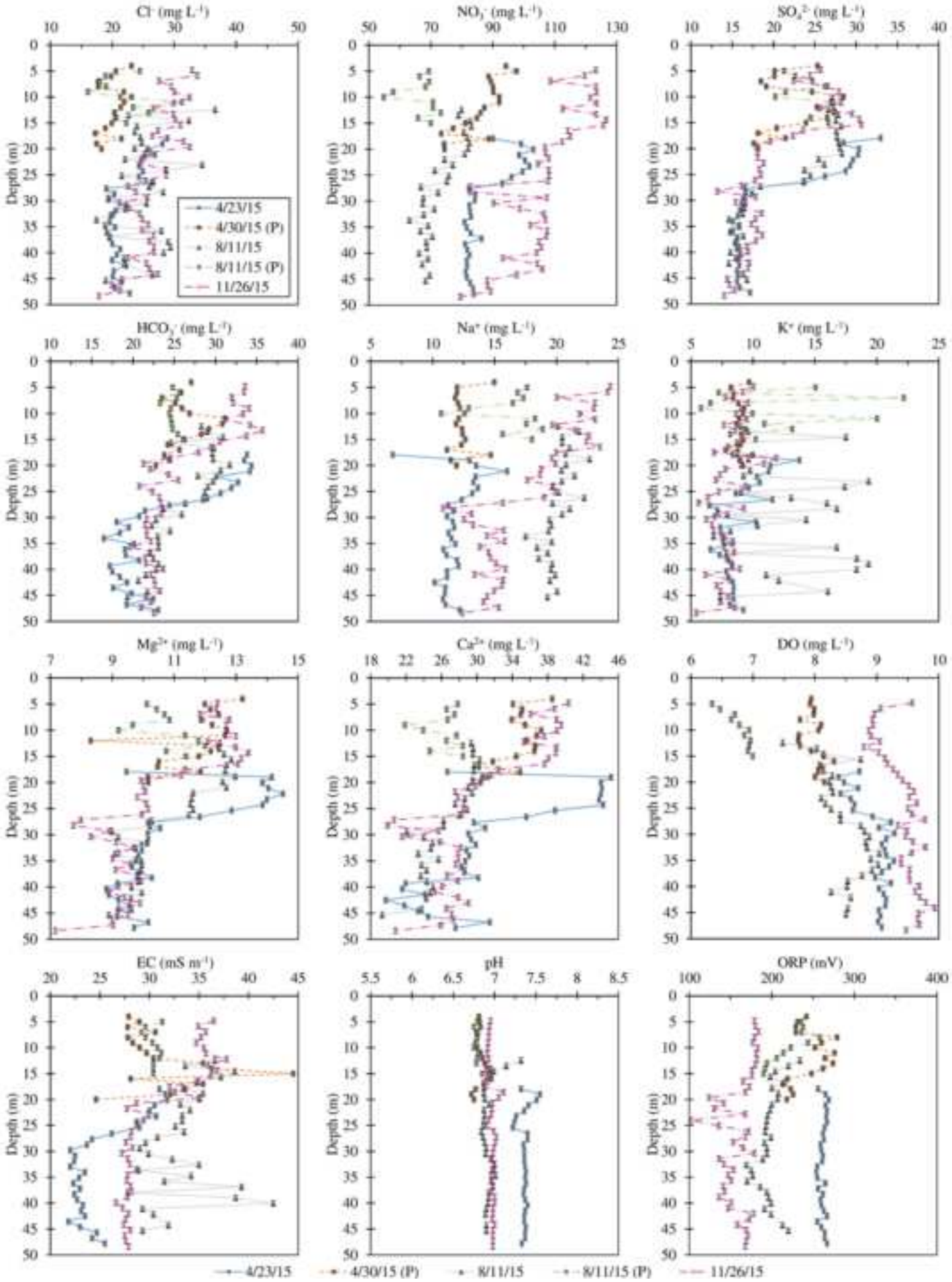
Cl⁻ (mg L⁻¹)
NO₃⁻ (mg L⁻¹)
SO₄²⁻ (mg L⁻¹)
HCO₃⁻ (mg L⁻¹)
Na⁺ (mg L⁻¹)
K⁺ (mg L⁻¹)
Mg²⁺ (mg L⁻¹)
Ca²⁺ (mg L⁻¹)
DO (mg L⁻¹)
EC (mS m⁻¹)
pH
ORP (mV)
Depth (m)
4/23/15
4/30/15 (P)
8/11/15
8/11/15 (P)
11/26/15

Figure 8

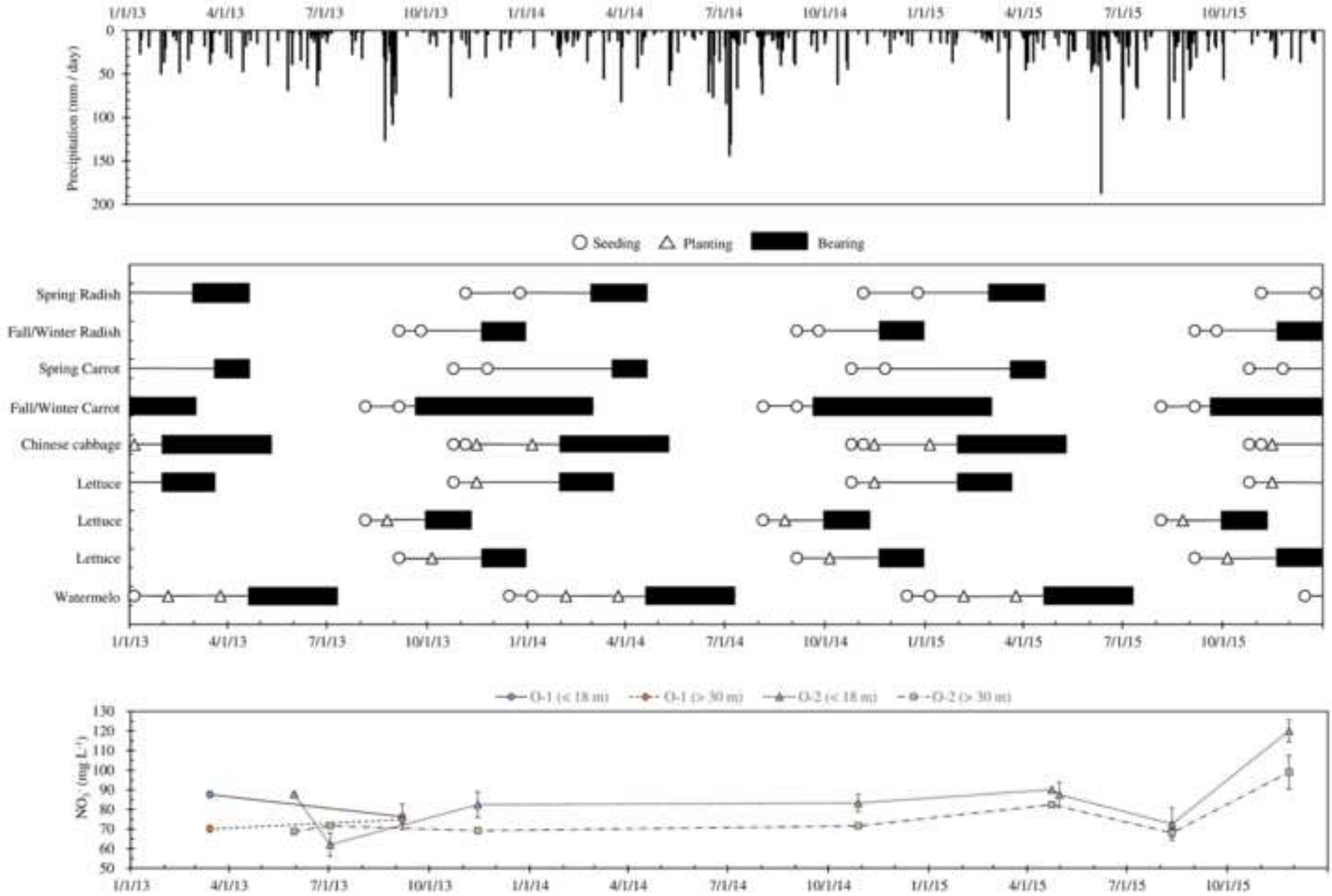
1/1/13
4/1/13
7/1/13
10/1/13
1/1/14
4/1/14
7/1/14
10/1/14
1/1/15
4/1/15
7/1/15
10/1/15
Precipitation (mm / day)
0
50
100
150
200
Seeding
Planting
Bearing
Spring Radish
Fall/Winter Radish
Spring Carrot
Fall/Winter Carrot
Chinese cabbage
Lettuce
Lettuce
Lettuce
Watermelo
O-1 (< 18 m)
O-1 (> 30 m)
O-2 (< 18 m)
O-2 (> 30 m)
NO3- (mg L-1)
130
120
110
100
90
80
70
60
50

Figure 9

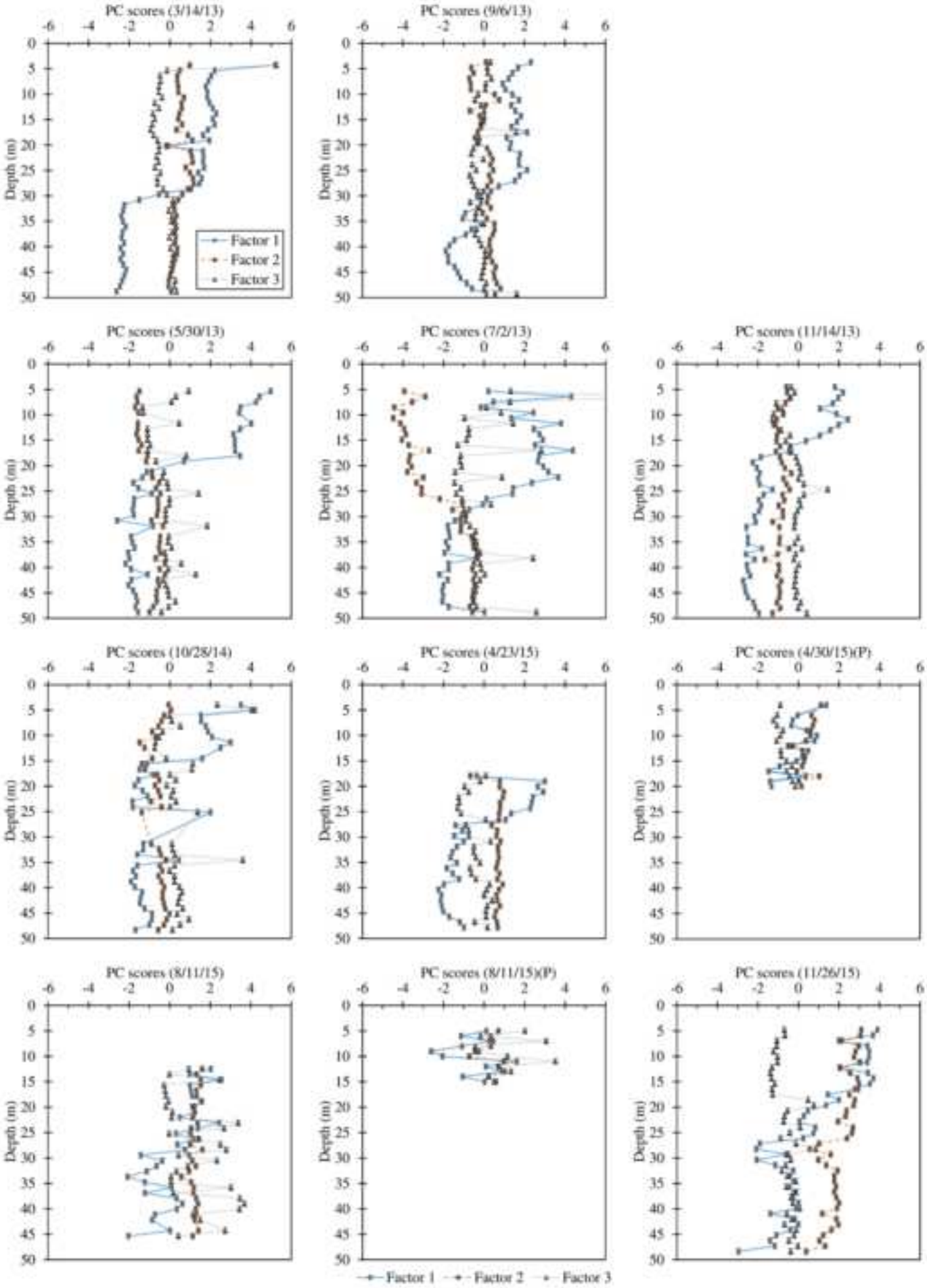
PC scores (3/14/13)
PC scores (9/6/13)
PC scores (5/30/13)
PC scores (7/2/13)
PC scores (11/14/13)
PC scores (10/28/14)
PC scores (4/23/15)
PC scores (4/30/15)(P)
PC scores (8/11/15)
PC scores (8/11/15)(P)
PC scores (11/26/15)
Depth (m)
Factor 1
Factor 2
Factor 3